NUCL SCI TECH (2017) 28:77
DOI 10.1007/s41365-017-0226-7

Radiation graft of acrylamide onto polyethylene separators for lithium-ion batteries

Xiao-Li Miao[1,2] · Ji-Hao Li[1] · Qun Xiang[2] · Jia-Qiang Xu[2] · Lin-Fan Li[1] · Jing-Ye Li[1]

Received: 2 March 2016 / Revised: 25 November 2016 / Accepted: 19 January 2017 / Published online: 28 April 2017

Abstract To improve the affinity between separators and electrolyte in lithium-ion battery, microporous polyethylene (PE) separator was grafted of polyacrylamide (PAAm) by radiation. Chemical structure of the PAAm-grafted PE separators (denoted as PE-g-PAAm) was characterized by Fourier transform infrared spectroscopy and X-ray photoelectron spectroscopy. Properties of the pristine PE and PE-g-PAAm were tested by scanning electron microscope, liquid electrolyte uptake and lithium-ion conductivity. Electrochemical performances of the grafted PE separators (up to 0.76×10^{-3} S/cm of ionic conductivity at room temperature) were much better than pristine PE, and performance of the battery with the grafted separator behaved better than with the virgin PE separator, under the same condition (assembled in Ar-filled glove box).

Keywords Lithium-ion battery · Polyethylene · Acrylamide · Irradiation graft · Separator

1 Introduction

Lithium-ion battery is the most commonly used portable powers for electronic products, due to its excellent performance in safety, long life span, high energy density, and so on [1–4], and the past years witnessed rapid performance improvements in lithium-ion battery. A lithium-ion battery consists of separator, anode, liquid electrolyte and cathode [5, 6]. As a crucial part of a battery, the separator maintains electrodes isolation of opposite polarities while it provides a pathway for lithium-ionic transportation. A typical separator usually has ionic conductivity, dimensional and mechanical stability, high electrolyte wettability, sufficient physical strength and thermal property and easiness for cell assembling [7]. Most commercialized polyolefin porous membranes, specifically polyethylene and polypropylene (PP), are preferable in lithium-ion battery production, due to their high chemical resistance, good thermal stability and low price. However, inherent hydrophobic property and low porosity (45%) of the separator usually caused poor wettability with organic electrolyte, resulting in poor stability of entrapped liquid electrolyte and corresponding low ion conductivity [8–10].

Radiation-induced graft polymerization is a well-known method for modification of polymeric material [11–14], without changing mechanical properties. And, being free of catalysts or additive, it is environmental-friendly [13].

Polyacrylamide (PAAm), as a biocompatible water-soluble polymer, is widely used as a polymeric flocculent in wastewater treatment [15]. Copolymerization of AAm with radiation grafting onto different substrates has attracted many researchers [16]. Gupta et al. [17] investigated the effects of solvents on radiation-induced graft copolymerization of acrylamide onto PE films and found

---

This work was supported by National Science Foundation of China (Grants 11575277, 11175234, 11505270, 51473183 and 11475246).

✉ Lin-Fan Li
lilinfan@sinap.ac.cn

✉ Jing-Ye Li
jingyeli@sinap.ac.cn

[1] Shanghai Institute of Applied Physics, Chinese Academy of Science, Shanghai 201800, People's Republic of China

[2] Department of Chemistry, College of Science, Shanghai University, Shanghai 200444, People's Republic of China

acetone, unlike methanol, did not behave inhibitory action on the grafting. Aliev [18] studied polyethylene's hydrophilicity and surface energy modified by radiation grafting of acrylamide and found that maximum value of the surface energy (46.5 mN/m) could reach ~15% of the PAAm content. However, to the authors' knowledge, little about the electrochemistry or even the battery has been reported. In this paper, we study PAAm-grafted PE separator to improve the affinity between nonaqueous electrolytes and electrodes, and to provide a convenient and effective way to introduce PAAm onto the surface of PE separator.

2 Experimental section

2.1 Materials

PE separator was donated from WIDE Company, Korea. Acrylamide (AAm, purity >99%) was purchased from J&K Chemical Ltd. Liquid electrolyte, 1 M $LiPF_6$ in ethylene carbonate/dimethyl carbonate (EC/DMC, 1:1 v/v), was supplied by Beijing Institute of Chemical Reagents and stored in Ar atmosphere. All reagents were used without purification.

2.2 Surface modification of PE separators

We prepared grafted PE separator by co-irradiation-induced graft polymerization technique. Strips of PE separators were soaked in acetone to clean the surface, vacuum-dried at 60 °C and weighed. AAm solution was prepared by adding the AAm monomer and 0.5 wt% $CuSO_4 \cdot 5H_2O$ into methanol under stirring. The $CuSO_4 \cdot 5H_2O$ was used as inhibitor in the reaction. Then, the weighed PE strips were immersed into the solution. Under the nitrogen gas protection, the mixture was irradiated by γ-ray in a ^{60}Co source at a dose rate of 0.49 Gy/s for 17 h. The grafted separators were washed thoroughly and soaked overnight with hot distilled water to ensure extraction of residual monomers and homopolymers. After that, the strips were dried at 60 °C for 24 h and weighed.

2.3 Characterization of separators

The degree of grafting (DG) is defined as:

$$\mathrm{DG} = [(W_1 - W_0)/W_0] \times 100\%, \tag{1}$$

where W_0 and W_1 are the weight of PE and PE-g-PAAm separators, respectively.

Structural changes of the separators were evaluated by Fourier transform infrared (FTIR) spectroscopy on a Nicolet Avatar 370 FTIR spectrometer by the culmination of 32 scans, at a resolution of 4 cm^{-1}, and X-ray photoelectron spectroscopy (XPS) on a Kratos Axis Ultra instrument, with monochromatic Al Kα ray, using wide scans in the range of 1100–0 eV and narrow scans for the C1s region. Scanning electron microscope (SEM) images of the separators were taken on a Hitachi SEM (S-4800, Japan) after sputtering gold on the sample. The voltage was 25 kV, and the current was 10 mA. Differential scanning calorimetry (DSC) test was conducted with a DSC Q100 system of TA instrument under nitrogen atmosphere at a heating rate of 10 °C/min. The degree of crystallinity (X_c) is calculated by Eq. (2):

$$X_c = (\Delta H_m/\Delta H_{100}) \times 100\%, \tag{2}$$

where ΔH_m is the heat of melting sample obtained from the peak area, and ΔH_{100} is the heat of melting of 100% crystalline PE polymer, which is 288.0 kJ/kg [19].

Liquid electrolyte uptake (ΔW) of separators was calculated by weight changes of separators. We used the tissue to remove the excess liquid electrolyte sticking to the surface of separator quickly before weighing.

$$\Delta W = [(W_b - W_a)/W_a] \times 100\%, \tag{3}$$

where W_a and W_b are the weight of samples before and after the 24-h soaking at room temperature, respectively.

The separators were immersed in the liquid electrolyte and then clipped by two platinum electrodes for measuring ionic conductivity (σ), which is calculated by Eq. (4). The impedance (R_b) was obtained by measuring AC impedance analysis from electrochemical work station system (CHI66d) at 30–70 °C over a frequency range of 1–10^5 Hz at 5 mV.

$$\sigma = d/(R_b A), \tag{4}$$

where d and A are the thickness and effective area of the separator, respectively.

To investigate the cycle performance, the coin cells assembled as $LiCoO_2$ (cathode)/separator–liquid electrolyte/lithium (anode) were tested on the cycle instrument (LAND, China) at room temperature, in the voltage range of 2.8–4.15 V. The specific capacity (D) is calculated by Eq. (5):

$$D = C/M, \tag{5}$$

where C is capacity of the tested battery and M is weight of the $LiCoO_2$ on the cathode sheet.

3 Results and discussion

3.1 Graft polymerization study

As shown in Fig. 1, the DG increased with the AAm concentration. Before AAm concentration of 6.2 wt%, DG

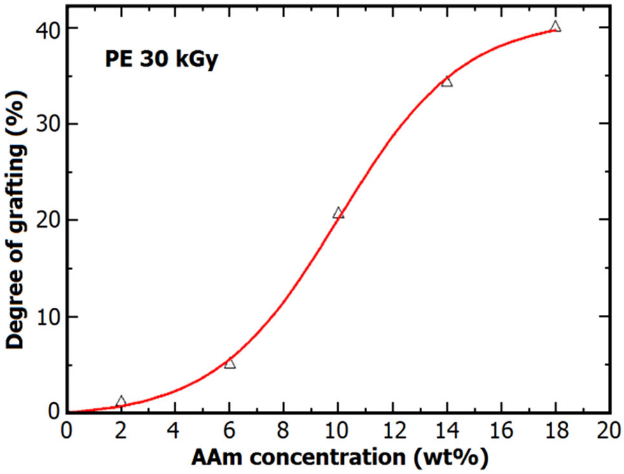

Fig. 1 Effects of mass fraction of AAm on DG of PE-g-PAAm separators. (Color figure online)

increased to 5.1% slowly, as there was only a small quality of PAAm in the system. Then, the DG increased rapidly, reaching 33.6% at AAm concentration of 14.2 wt%, where the DG increase became slowly again, toward a level of saturation. These can be explained as follows: With two kinds of radical in the system, there was a competition between grafting reaction and copolymerization; when the AAm concentration was below 14.2 wt%, the grafting prevailed; while the copolymerization grew stronger with more AAm, the system became viscous gradually, which further hampered the grafting [20].

3.2 FTIR and XPS characterizations

Surface chemical compositions of the PE and PE-g-PAAm separators were analyzed by FTIR and XPS spectroscopy. The FTIR spectra of the pristine PE and PE-g-PAAm separators of various DGs are shown in Fig. 2a. After grafting, new peaks at 3417 and 3347 cm^{-1} were identified as the asymmetric and symmetric stretching vibration bands of the N–H group, and the new bands at 3197 and 1712 cm^{-1} stood for C(O)-NH$_2$ and C=O stretching vibration of grafted PAAm. The peak intensities increased with DG, indicating that PAAm chains were grafted onto the surface successfully [15].

Figure 2b shows the C1s wide-scan XPS spectra for the pristine PE and PE-g-PAAm separator (DG 22.6%). There were only C and O in pristine PE, while N appeared in PE-g-PAAm separator, an indication of PAAm graft onto the PE separator. The tiny amount of O in pristine PE separator may be the surfactant that was not informed by the supplier.

The XPS core-level spectra for the pristine PE and PE-g-PAAm separator (DG 22.6%) are shown in Fig. 3. The PE spectra had just one peak at 284.8 eV, which was the overlap of CH$_2$ and CH$_2$-CH$_2$ groups. In the PE-g-PAAm spectra, two new peaks at 286.8 and 288.2 eV were attributed to the amide groups [15]. The FTIR and XPS results indicate that PAAm graft chains are combined to the PE chain by chemical bonds.

3.3 Morphologies of the separators

SEM images (Fig. 4) show that both the pristine separator and grafted separators of different DGs had many open pores distributed uniformly. The PAAm-grafted separators retain their microporous net structure, but the microporous structure of PE-g-PAAm 45.9% became worse apparently.

3.4 Thermal properties

Thermal properties of PE and PE-g-PAAm separators of different DGs measured by DSC are given in Fig. 5 and Table 1. The thermograms of pristine and grafted separators remained almost homologous, but the intensity of

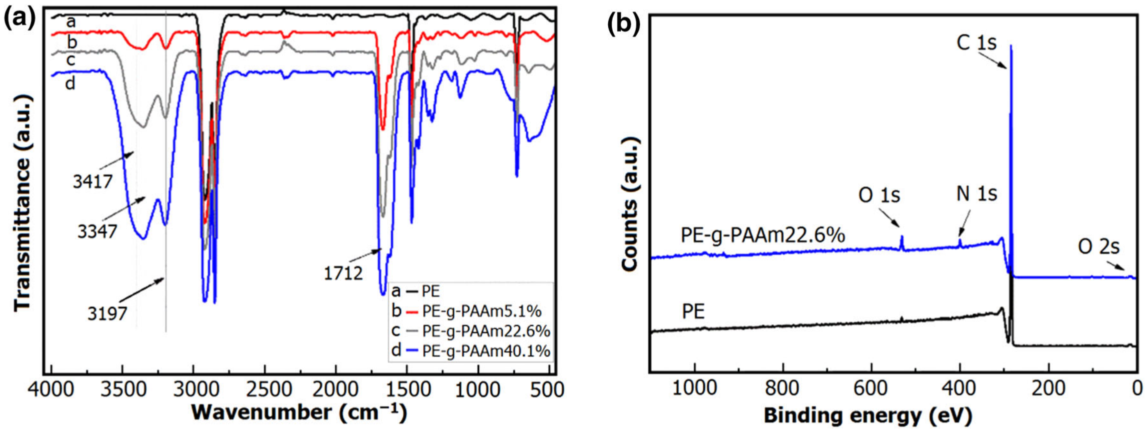

Fig. 2 FTIR (**a**) and XPS (**b**) spectra of the pristine PE and PE-g-PAAm separators of different DGs. (Color figure online)

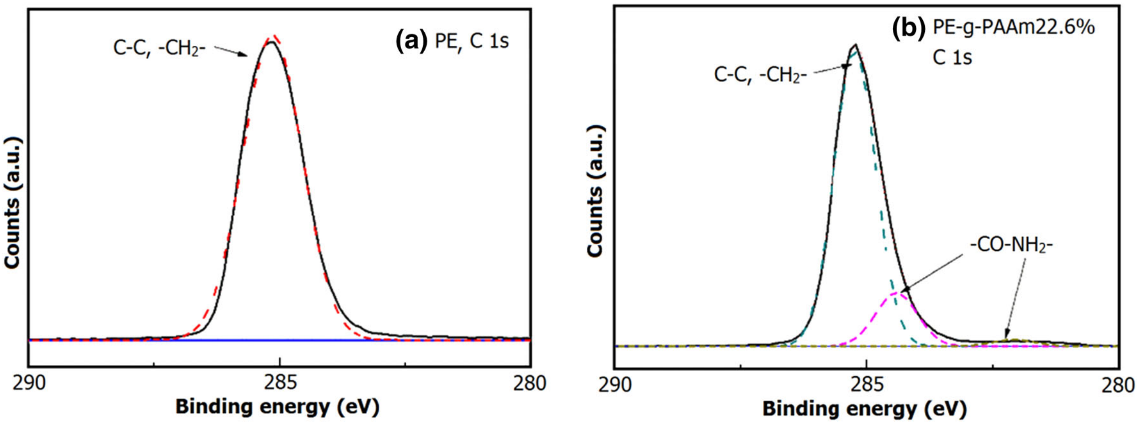

Fig. 3 C1s spectra of **a** pristine PE separator and **b** PE-g-PAAm separator with DG of 22.6%. (Color figure online)

Fig. 4 SEM images of pristine PE separator (**a**) and PE-g-PAAm separators of DG being 16.7% (**b**), 33.6% (**c**) and 45.9% (**d**)

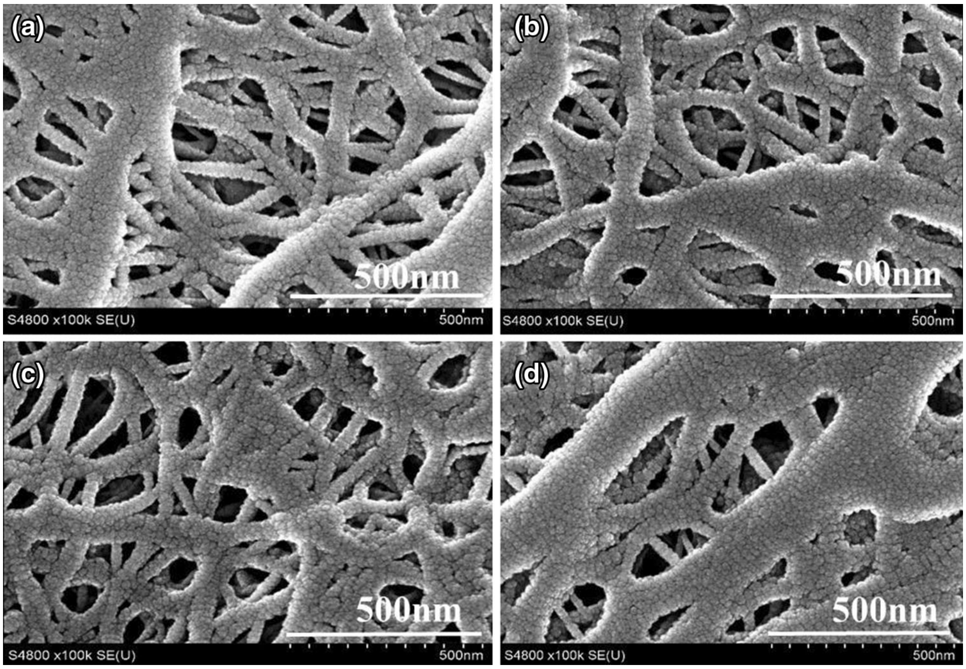

peaks decreased with increasing DGs. Also, the onset, peak and degree of crystallinity decreased with increasing DGs. The reduction in the degree of crystallinity upon grafting of PAAm corresponded to the dilution of PE crystalline zone with the amorphous PAAm and the partial disruption in the crystalline structure of PE separator.

3.5 Liquid electrolyte uptake

The affinity to electrolyte is a key property of a separator, and higher uptake means more electrolyte contained in separator. The uptake of electrolyte is shown in Fig. 6. As we know, the porosity and the content of active component of separator are the factors that determine the electrolyte uptake [1]. The uptake increased with the DG and rose to 688.4% at DG = 22.6%, where it began to decrease. This maximum increase is almost 2.8 times of the pristine PE (245.0%), because the polar functional groups of the grafted PAAm can greatly improve the affinity between the separator and electrolyte and hence the increase in electrolyte uptake [21]. When DG was greater than 22.6%, too many separator pores were occupied by the grafted chains, which hindered the swelling of the separators and resulted in the decreasing uptake.

3.6 The lithium-ion conductivity of the separators

Lithium-ion conductivities of the pristine PE separator and PE-g-PAAm separators of different DGs, as function of temperature, are shown in Fig. 7. Generally, ionic conductivity is

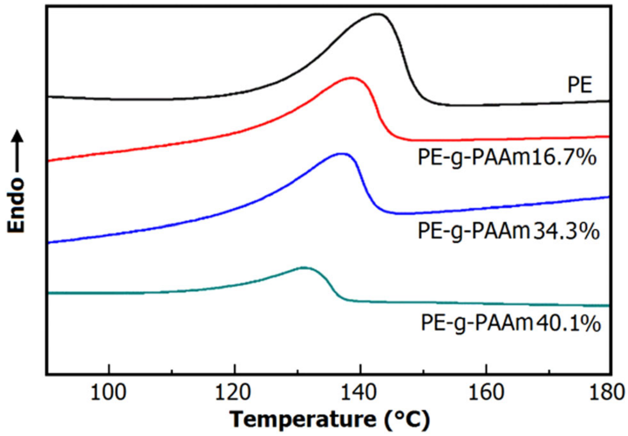

Fig. 5 DSC curves of PE and PE-g-PAAm separators with different DGs. (Color figure online)

Table 1 DSC data of pristine PE separator (a) and PE-g-PAAm 16.7% (b), 34.3% (c) and 40.1% (d)

Samples	Onset (°C)	Peak (°C)	$\triangle H$ (J/g)	Crystallinity (%)
a	124.38	139.20	131.11	69.74
b	122.76	138.35	79.51	42.30
c	118.13	133.59	65.11	34.63
d	116.36	131.29	36.06	19.18

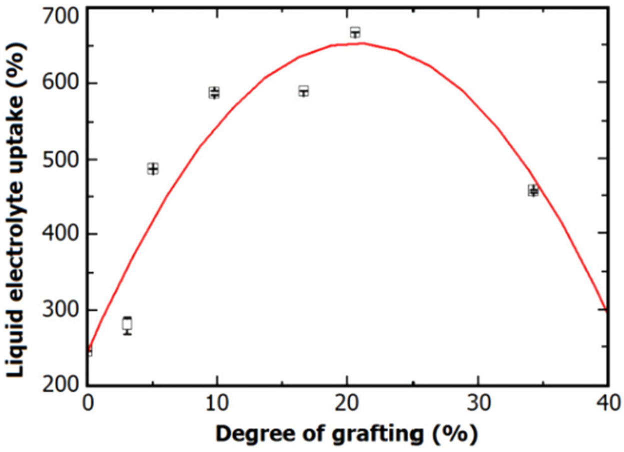

Fig. 6 Liquid electrolyte uptake of PE-g-PAAm separators of different DGs. (Color figure online)

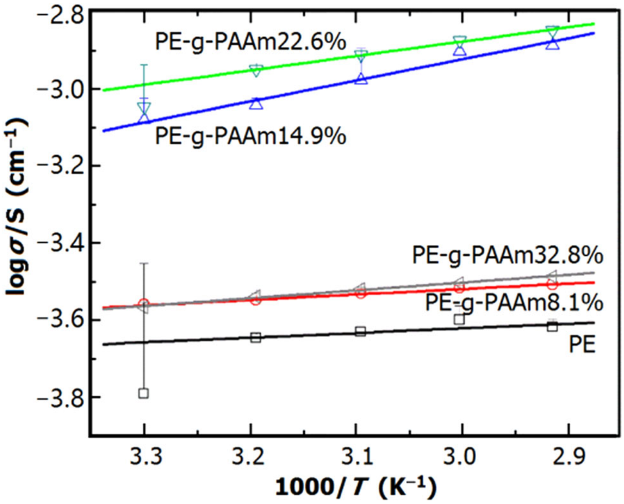

Fig. 7 Lithium-ion conductivities of pristine PE separator and PE-g-PAAm separators of different DGs, as function of temperature. (Color figure online)

influenced by the active component and the mobility of lithium ions [22]. Uncovered open pores, good connectivity of separators, and high amount of lithium ions, which depends on the high electrolyte uptake, can make sense of lithium-ion mobility and improve ion conductivity [1]. At DGs $\leq$22.6%, the electrolyte contained in the separators, and their conductivity, increased with DG, as the grafted PAAm improved affinity between separators and electrolyte. When the DG was too high, the pores were blocked by the PAAm, resulting in less capacity of electrolyte. Also, high amount of PAAm formed highly viscous gel matrix, the mobility of lithium ions decreased, and so did the ionic conductivity. In Fig. 7, the conductivity increased with temperature, because at high temperatures, the activity of Li^+ surged, and the conductivity of lithium ion was improved. The performance of PE-PAAM 22.6% was the highest in conductivity, being 0.76×10^{-3} S/cm at 30 °C, four times more than the pristine PE separator (0.15×10^{-3} S/cm).

3.7 The cycling performance of lithium-ion battery

Figure 8a, b shows the first, tenth and twentieth cycles of charge–discharge performance of the cell assembled with PE-g-PAAm 22.6% separators. The first cycle specific capacity of the PE-g-PAAm cell was 121.9 mA h/g, while it was 117.8 mA h/g for the pristine PE cell. The charge–discharge capacities of the cells as a function of the cycle number are shown in Fig. 8c, which were performed at 0.1 C rate, evaluated at an operating voltage of 4.15–2.8 V. After 20 cycles, the charge and discharge capacity retention ratios of the PE-g-PAAm cell were 85.3 and 93.0%, respectively, while those of the pristine PE cell were 67.9 and 73.8%, respectively. The improvements can be attributed to the PAAm gel layer, which entraps more electrolyte so that more lithium ions are yielded to anticipate electrochemical reaction, and promotes more intimate contact between electrode and separators, so as to restrain the growth of SEI film, lower the impendence on the electrode and finally suppress the lithium-ion consumption [23, 24].

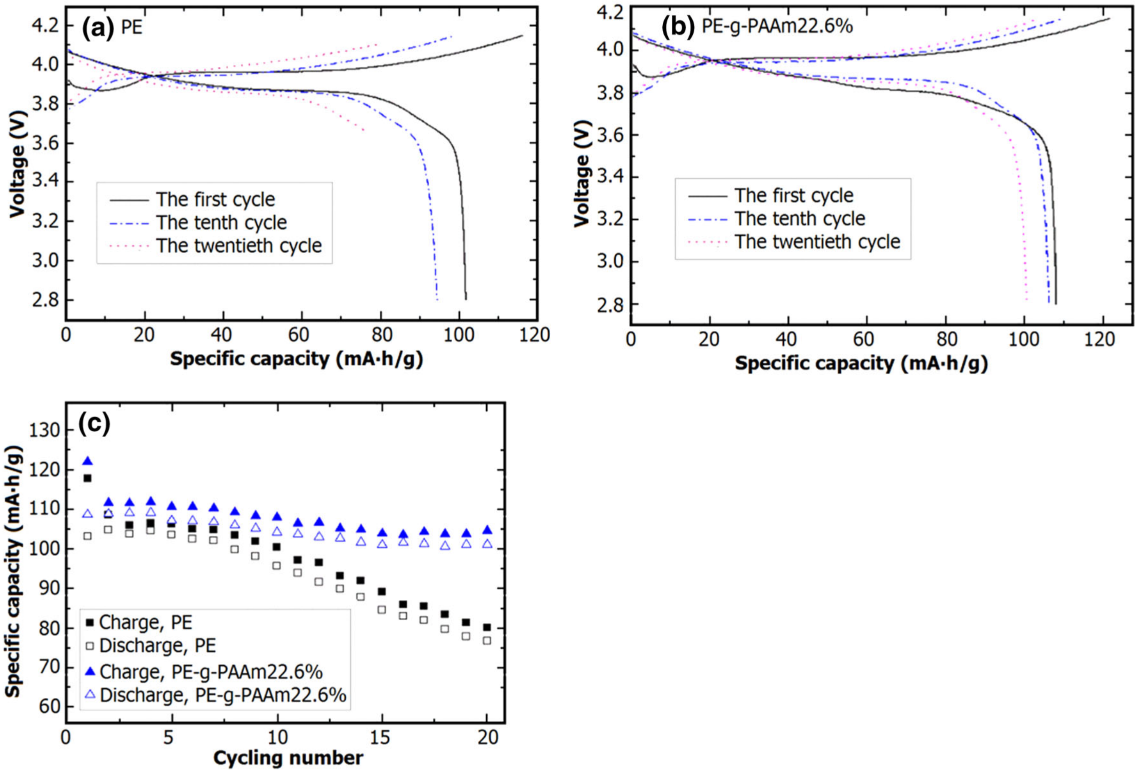

Fig. 8 Charge–discharge specific capacity of PE (**a**) and PE-g-PAAm 22.6% (**b**) separators, and the cells assembled with them (**c**). (Color figure online)

4 Conclusions

Polyacrylamide chains are grafted onto PE separators by the co-irradiation grafting method, which is thought of a universe way to modify other separators, with advantages against pre-irradiation. PAAm introduction onto PE separator improves the compatibility with liquid electrolyte, with increased electrolyte uptake and ionic conductivity, being 0.76×10^{-3} S/cm at room temperature for the PE-g-PAAm 22.6% sample, four times as much as the pristine PE separators. The cycle performance of the assembled lithium-ion cell is improved, too. The PAAm grafting onto separator is a promising way for application in LIBs.

References

1. L.F. Fang, J.L. Shi, B.K. Zhu et al., Facile introduction of polyether chains onto polypropylene separators and its application in lithium ion batteries. J. Membr. Sci. **448**, 143–150 (2013). doi:10.1016/j.memsci.2013.07.065
2. K. Gregorczykand, M. Knez, Hybrid nanomaterials through molecular and atomic layer deposition: top down, bottom up, and in-between approaches to new materials. Prog. Mater. Sci. **75**, 1–37 (2016). doi:10.1016/j.pmatsci.2015.06.004
3. P. Zhang, L. Chen, C. Shi et al., Development and characterization of silica tube-coated separator for lithium ion batteries. J. Power Sources **284**, 10–15 (2016). doi:10.1016/j.jpowsour.2015.02.126
4. R. Zhao, S. Zhang, J. Liu et al., A review of thermal performance improving methods of lithium ion battery: electrode modification and thermal management system. J. Power Sources **299**, 557–577 (2015). doi:10.1016/j.jpowsour.2015.09.001
5. J.L. Shi, L.F. Fang, H. Li et al., Improved thermal and electrochemical performances of PMMA modified PE separator skeleton prepared via dopamine-initiated ATRP for lithium ion batteries. J. Membr. Sci. **437**, 160–168 (2013). doi:10.1016/j.memsci.2013.03.006
6. G.L. Zhu, K.C. Wen, W.Q. Lv et al., Materials insights into low-temperature performances of lithium-ion batteries. J. Power Sources **300**, 29–40 (2015). doi:10.1016/j.jpowsour.2015.09.056
7. P. Arora, Z.M. Zhang, Battery separators. Chem. Rev. **104**, 74419–74462 (2014). doi:10.1021/cr020738u
8. J. Chen, S. Wang, L. Ding et al., Performance of through-hole anodic aluminum oxide membrane as a separator for lithium-ion battery. J. Membr. Sci. **461**, 22–27 (2014)
9. H. Li, H. Zhang, Z.Y. Liang et al., Preparation and properties of poly(vinylidene fluoride)/poly(dimethylsiloxane) graft (poly(propylene oxide)-block-poly(ethylene oxide)) blend porous separators and corresponding electrolytes. Electrochim. Acta **116**, 413–420 (2014). doi:10.1016/j.electacta.2013.11.076
10. B.A. Zhang, F.Y. Kang, J.M. Tarascon et al., Recent advances in electrospun carbon nanofibers and their application in electrochemical energy storage. Prog. Mater. Sci. **76**, 319–380 (2016). doi:10.1016/j.pmatsci.2015.08.002

11. H. Ma, S. Yao, J. Li et al., A mild method of amine-type adsorbents syntheses with emulsion graft polymerization of glycidyl methacrylate on polyethylene non-woven fabric by pre-irradiation. Radiat. Phys. Chem. **81**, 1393–1397 (2012). doi:10.1016/j.radphyschem.2011.11.042
12. R. Cai, B. Deng, H.Q. Jiang et al., Radiation induced graft polymerization of a fluorinated acrylate onto fabric. Radiat. Phys. Chem. **81**, 1354–1356 (2012). doi:10.1016/j.radphyschem.2011.11.050
13. J.E. Martin-Alfonso, J.M. Franco, Influence of polymer reprocessing cycles on the microstructure and rheological behavior of polypropylene/mineral oil oleogels. Polym. Test. **45**, 12–19 (2015). doi:10.1016/j.polymertesting.2015.04.016
14. F. Zhang, W. Zhang, Y. Yu et al., Sol–gel preparation of PAA-g-PVDF/TiO2 nanocomposite hollow fiber membranes with extremely high water flux and improved antifouling property. J. Membr. Sci. **432**, 25–32 (2013). doi:10.1016/j.memsci.2012.12.041
15. X.X. Yang, B. Deng, Z.Y. Liu et al., Microfiltration membranes prepared from acryl amide grafted poly(vinylidene fluoride) powder and their pH sensitive behaviour. J. Membr. Sci. **362**, 298–305 (2010). doi:10.1016/j.memsci.2010.06.057
16. E.M. El-Nesr, Gamma radiation induced graft copolymerization of acrylamide onto EPDM blended with PE. Polym. Adv. Technol. **13**, 626–635 (2002). doi:10.1002/pat.262
17. B. Gupta, N. Anjum, A.P. Gupta, Influence of solvents on radiation-induced graft copolymerization of acrylamide into polyethylene films. J. Appl. Polym. Sci. **77**(6), 1401–1404 (2000). doi:10.1002/1097-4628(20000808)77:6<1401:Aid-App28>3.0.Co;2-T
18. R. Aliev, Hydrophilicity and surface energy of polyethylene modified by radiation grafting of acrylamide. Polym. Bull. **47**, 99–104 (2001). doi:10.1007/s002890170026
19. J.A. Reyes-Labarta, M.M. Olaya, A. Marcilla, DSC and TGA study of the transitions involved in the thermal treatment of binary mixtures of PE and EVA copolymer with a crosslinking agent. Polymer **47**, 8194–8202 (2006). doi:10.1016/j.polymer.2006.09.054
20. J. Wu, J. Li, B. Deng et al., Self-healing of the superhydrophobicity by ironing for the abrasion durable superhydrophobic cotton fabrics. Sci. Rep. **3**, 2951 (2013). doi:10.1038/srep02951
21. S.J. Gwon, J.H. Choi, J.Y. Sohn et al., Radiation grafting of methyl methacrylate onto polyethylene separators for lithium secondary batteries. Nucl. Instrum. Methods Phys. Res. Sect. B **266**, 3387–3391 (2008)
22. K. Gao, X. Hu, T. Yi et al., PE-g-MMA polymer electrolyte membrane for lithium polymer battery. Electrochim. Acta **52**, 443–449 (2006)
23. S.J. Gwon, J.H. Choi, J.Y. Sohn et al., Battery performance of PMMA-grafted PE separators prepared by pre-irradiation grafting technique. J. Ind. Eng. Chem. **15**, 748–751 (2009). doi:10.1016/j.jiec.2009.09.057
24. H.S. Jeong, S.Y. Lee, Closely packed SiO_2 nanoparticles/poly(vinylidene fluoride-hexafluoropropylene) layers-coated polyethylene separators for lithium-ion batteries. J. Power Sources **196**, 6716–6722 (2011)